Bull. Mater. Sci., Vol. 40, No. 1, February 2017, pp. 247–251. © Indian Academy of Sciences.
DOI 10.1007/s12034-016-1354-0

Impact of divalent dopant Ca^{2+} on the electrical properties of ZnO by impedance spectroscopy

TANUSHREE DAS, BIKRAM KESHARI DAS, S K S PARASHAR and KAJAL PARASHAR*
School of Applied Sciences, Nanosensor Lab, KIIT University, Bhubaneswar 751024, India

MS received 1 April 2016; accepted 10 June 2016

Abstract. **The electrical properties of $Zn_{1-x}Ca_xO$ ($x = 0$, 0.01, 0.02 and 0.03) nanoceramics synthesized by solid-state reaction method were investigated by complex impedance spectroscopy (CIS) from room temperature to 500°C. Structural analysis of the synthesized material using the X-ray diffraction technique suggests that they exhibit a single phase with hexagonal wurtzite structure. Experimental results indicate that the synthesized material shows temperature-dependent relaxation phenomena. The variation of frequency exponent (s) with temperature shows the presence of thermally activated polarization mechanism in the synthesized sample. Dielectric constant was found to decrease with increase in frequency and temperature for Ca-doped samples. Ca-doped ZnO sample shows dielectric loss at lower temperature than that of pure ZnO.**

Keywords. **XRD; $Zn_{1-x}Ca_xO$; impedance spectroscopy.**

1. Introduction

ZnO is a technologically important semiconducting material having unique physical and chemical properties. A wide and direct band (0.37 eV), large exciton binding energy (60 meV), high electron mobility and high thermal conductivity make it suitable for a wide range of device applications [1]. The study of the electrical properties of ZnO nanostructures led to their future application in nanoelectronics. The electrical properties of ZnO result from point native defects as oxygen vacancies (V_O) and zinc interstitials (Zn_i^+) [2]. Generally, the electrical properties of a nanostructure material depends on high surface to volume ratio of grains, small size, enhanced contribution from grain and grain boundaries, band structure modification, defects and quantum confinement of charge carriers [3]. A relatively small change in concentration of native point defects and impurities (down to 10^{-14} cm^{-3} or 0.01 ppm) significantly affects the electrical and optical properties of ZnO [1]. Doping is a suitable and facile method to tune the electrical, optical, magnetic, piezoelectric and electronic properties of ZnO [4]. Doping of Ca in ZnO is important for biological [5], optical [6], sensing [7] and photonics [8] applications.

Complex impedance spectroscopy (CIS) is a powerful method of characterizing electrical properties of a material and their interfaces with electronically conducting electrodes [9]. It is employed to analyse the properties of intragranular, interfacial regions and their dependence on variables like temperature, frequency and applied static voltage [10]. This analysis provides a correlation between the structural and electrical properties of a material in a wide range of frequencies and temperature.

Plenty of reports are available for transition metal, nonmetal and rare-earth-doped ZnO for different applications. However in literature, the work on alkaline-earth-metal-doped ZnO is limited. It seems from literature survey that impedance analysis and detailed electrical characterization of this material received very little attention. In view of this, the current study involves the synthesis of Ca-doped ZnO nanoceramics ($Zn_{1-x}Ca_xO$) by solid-state reaction method and detailed electrical properties investigated by impedance spectroscopy for useful nanoelectronics applications.

2. Experimental

ZnO doped with Ca, abbreviated as $Zn_{1-x}Ca_xO$ ($x = 0, 0.01$, 0.02 and 0.03), was prepared by solid-state reaction method. High purity precursor ZnO and $CaCO_3$ was weighted according to their atomic ratio, used as a raw material to achieve the desired product. The sample was prepared by thoroughly grinding these powders in an agate mortar to get the homogeneity. After grinding, the mixture was calcined at 900°C for 2 h with a heating rate of 2°C min^{-1}. The calcined powder mixed with PVA acts as a binder to prepare pellets. The pellets were sintered at 1000°C for 2 h in air atmosphere. In order to study the electrical properties, both the surfaces of the pellet were polished and electrode with high purity silver paint and dried at 700°C for 15 min.

The phase constitutes and crystal structure of the calcined sample was determined by X-ray diffraction (XRD) technique and the electrical properties of the sample pellet was analysed by using a computer-controlled impedance analyser (Hioki LCR Hi-tester-3532-50) starting from room

*Author for correspondence (kparasharfch@kiit.ac.in)

temperature to 500°C over a wide range of frequency (100 Hz–1 MHz).

3. Results and discussion

3.1 *Structural analysis*

The formation of the synthesized material was checked by XRD technique. The phase, crystal structure and lattice parameter of the calcined samples were obtained from the XRD patterns shown in figure 1.

All the peaks belong to hexagonal wurtzite structure of ZnO with space group $P6_3mc$ and matched with JCPDS: 36-1451. This confirms the complete solid solubility of Ca^{2+} ions into ZnO lattice. The prominent peaks in the XRD patterns are indexed to its respective *hkl* planes and the highest intensity peak is along the the plane (101). There is no evidence of secondary peak formation, which may be attributed to the incorporation of Ca^{2+} ion into the ZnO lattice rather than the interstitial ones. This also confirms the formation of single phase of the materials. All the reflection peaks were indexed and lattice parameters were obtained by a computer program POWDMULT shown in figure 2a and b. The crystallite sizes (D) of the prepared nanoceramic was estimated from the broadening of the reflection peaks using Scherrer's equation $D = 0.9\lambda/\beta\cos\theta$ [11] and are found to be 50 nm ($x = 0$), 34, 32 and 36 nm ($x = 0.01$, 0.02 and 0.03) respectively. The change in lattice parameters is due to the substitution of Ca^{2+} (0.99 Å), which has a larger ionic radius than that of Zn^{2+} (0.74 Å), in their sites with tetrahedral co-ordinates [12]. It can be observed from figure 2a and b that there is a jump of lattice parameter values for $x = 0.01$ in $Zn_{1-x}Ca_xO$ nanoceramics. Similar higher values of lattice parameter for Ca-doped ZnO have been reported by Bai *et al* [13]. Such kind of variation in lattice parameter for Ca-doped ZnO nanoceramics is related to the shifting of the most intense (101) XRD peaks towards lower and higher diffraction angles. The shifting of 2θ values for Ca-doped ZnO nanoceramics is clearly shown in figure 1b. From figure 1b, it can be seen that for $x = 0.01$, the (101) peak is shifted to lower 2θ values, showing an increase in the lattice parameter values [14,15], while shifting of peaks towards higher 2θ values indicates reduction of lattice parameter and cell volume [16]. This also provides indirect evidence that Ca^{2+} ion is incorporated into the crystal structure of ZnO [17]. Besides this no systematic variation in lattice parameter was observed with increase in concentration of Ca. Similar data were also reported for Ru-doped ZnO [18].

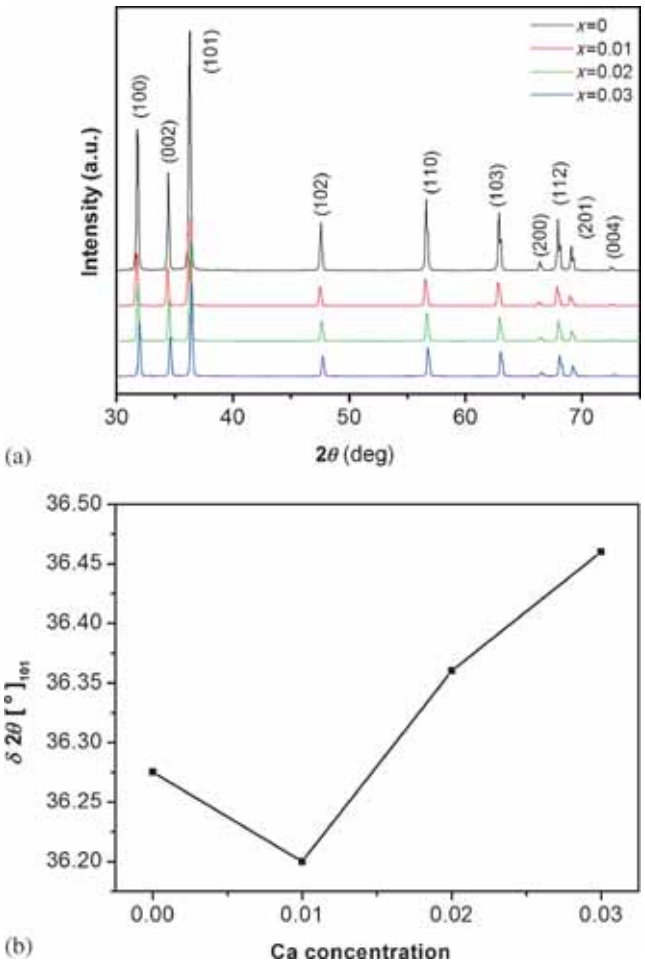

Figure 1. (**a**) XRD patterns of $Zn_{1-x}Ca_xO$ nanoceramics and (**b**) shifting of 2θ values with Ca concentration.

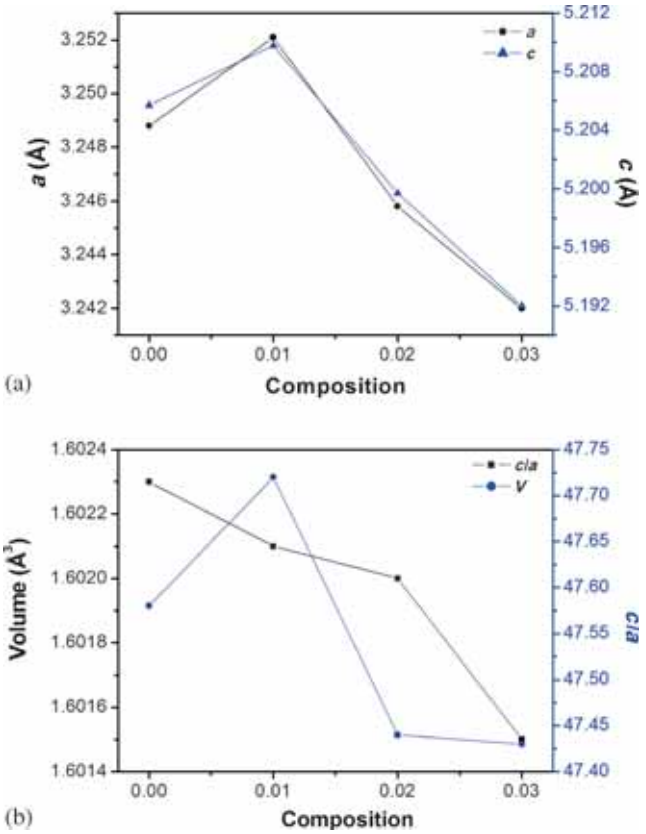

Figure 2. (**a**) Variation of lattice parameters a and c with composition of $Zn_{1-x}Ca_xO$ nanoceramics and (**b**) variation of volume and c/a ratio with composition of $Zn_{1-x}Ca_xO$ nanoceramics.

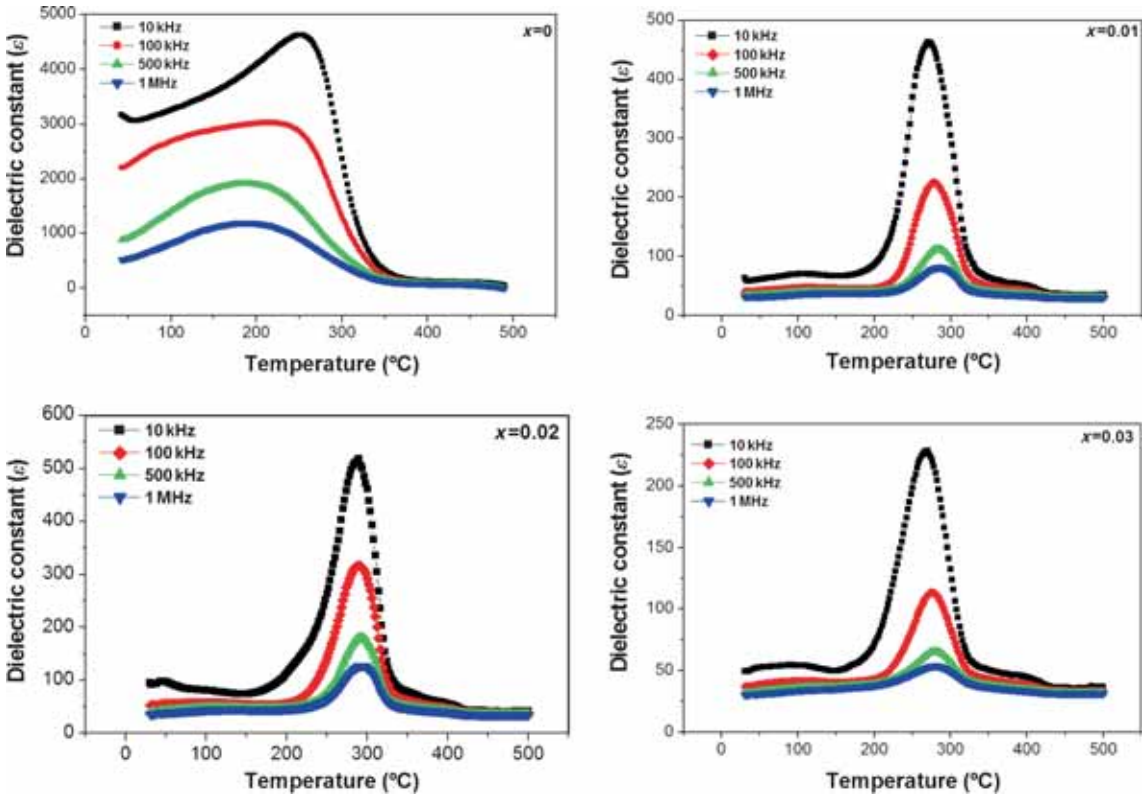

Figure 3. Temperature-dependent dielectric constant of $Zn_{1-x}Ca_xO$ nanoceramics at selected frequencies with different concentrations of Ca.

3.2 *Dielectric properties*

Figure 3 displays the variation of dielectric constant (ε) with temperature at different frequencies (10 kHz–1 MHz) of $Zn_{1-x}Ca_xO$ ($x = 0$, 0.01, 0.02 and 0.03) nanoceramics. From figure 3 it was observed that all the samples exhibit dielectric dispersion, where the dielectric constant decreases as the frequency increases. At low frequencies higher values of dielectric constant were observed due to interfacial/space polarization [19]. The dielectric constant increases with increase in temperature and attains a maximum value ε_{max} at transition temperature (T_c) and then decreases with further increase in temperature. Again, the dielectric constants for all the samples show a peak that is shifted to higher temperature as the frequency increases. These peaks appear when the jumping frequency of localized electron approximately becomes equal to that of the externally applied a.c. field. The shifting of these peaks with increase in frequency towards higher temperature can be attributed to the increase of the hopping frequency of the charge carriers [19]. It has been observed that the sharpness of peak decreases and it tends to be broadened with increase in frequency. Compared with pure ZnO ($x = 0$), Ca-doped ZnO has drastically decreased dielectric constant due to the inhibition of dipole rotation, which is caused by the substitution of Ca^{2+} ion into ZnO lattice.

Loss tangent (tan δ) represents the energy dissipation in the system. Figure 4 shows the variation in dielectric loss

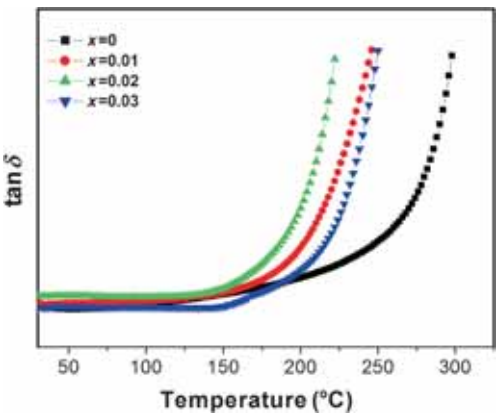

Figure 4. Temperature-dependent dissipation factor of $Zn_{1-x}Ca_xO$ nanoceramics.

factor with temperature at 10 kHz. At low temperature, the loss is linear but at higher temperature it is not linear and shows a significant increase, which is widely observed for ceramic materials due to space charge polarization [20]. Additionally, higher value of dielectric loss at higher temperature may be due to macroscopic distortion of charges [21]. This is a general trend where tan δ increases with increases in temperature and decreasing frequency [22]. It was observed that all samples have high dielectric loss near phase transition temperature. It is also noticeable that the loss is maximum when there is no doping but it decreases with Ca doping.

The increase in loss tangent is due to an increase in conduction of residual current as well as conduction current. This is caused by the dipole movement, which reaches its maximum at a certain definite temperature [23].

In ZnO, the process of electrical conduction may be due to the motion of ions in host crystal lattice. Such conduction is known as intrinsic and is particularly important at high temperature. On the other hand the electrical conduction in Ca-doped ZnO is due to the motion of relatively weakly bound ions. Ca^{2+} ions include impurity ions as well as ions located at defect of ZnO crystal lattice. The Ca^{2+} ions give rise to extrinsic impurity conduction of a crystal. Therefore, the motion associated with the motion of weakly bound ions may appear at relatively low temperature. From figure 3, it has been observed that T_c of ZnO increases with Ca doping. The increase of T_c with increase in concentration of Ca (up to $x = 0.02$) in turn shows the dielectric loss at low temperature. Therefore, there is a systematic variation of dielectric loss up to $x = 0.02$. However, for $x = 0.03$, the T_c again decreases, which shows the dielectric loss at higher temperature than those at $x = 0.01$ and 0.02.

3.3 *Impedance analysis*

The electrical behaviour of $Zn_{1-x}Ca_xO$ ($x = 0$, 0.01, 0.02 and 0.03) nanoceramics has been studied over a wide range of frequency, at room temperature using CIS. It describes the electrical processes occurring in a system by applying an a.c. signal as input perturbation, which helps separate the contribution of electroactive regions (such as grain boundary and bulk effects). The complex impedance of a system can be written as [24].

$$Z^* = Z' + jZ'',$$

where $Z' = Z\cos\theta$, $Z'' = Z\sin\theta$ and $j = \sqrt{-1}$.

Figure 5 shows the variation of imaginary part of impedance (Z'') with frequency at different temperatures. The graph shows that the value of Z'' reaches a maximum of Z''_{max} at all temperatures. For Ca-doped ZnO the value of Z''_{max} shifts to high frequency with increasing temperature and also a peak broadening exists in the system, indicating temperature-dependent electrical relaxation phenomena in the material [25]. The Z'' increased with increase in frequency in all the temperature ranges studied here and exhibited a maximum (Z''_{max}) before it started decreasing. The relaxation phenomenon in the material may be due to the presence of immobile species/electrons at low temperature and defects/vacancies at higher temperature [26]. The asymmetric broadening of the peaks suggested the presence of electrical change in the material with a spread of relaxation time [25]. The merging of Z'' values in the high-frequency region for Ca-doped ZnO may be an indication of the accumulation of space charge in the material. Furthermore, it is noticed that with the increase in temperature the magnitude of Z'' decreases, the effect being more pronounced at the peak position. For ZnO the frequency-dependent imaginary

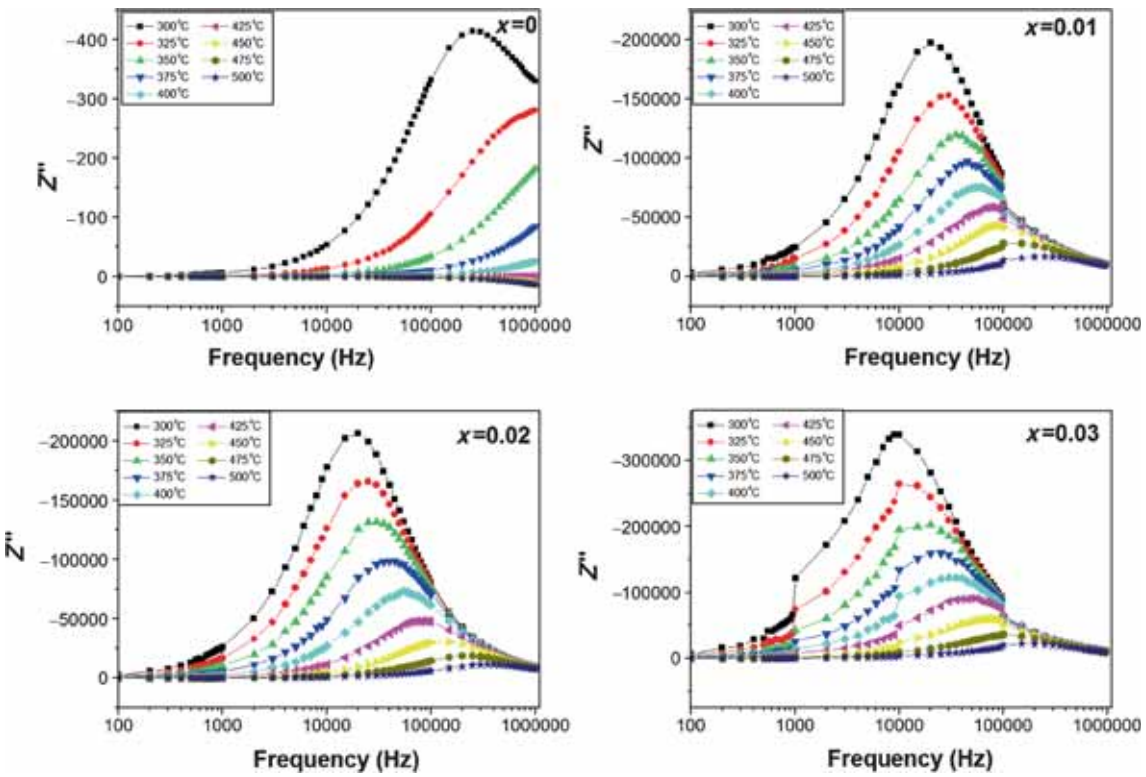

Figure 5. Frequency-dependent variation of imaginary part (Z'') for $Zn_{1-x}Ca_xO$ nanoceramics at different temperatures.

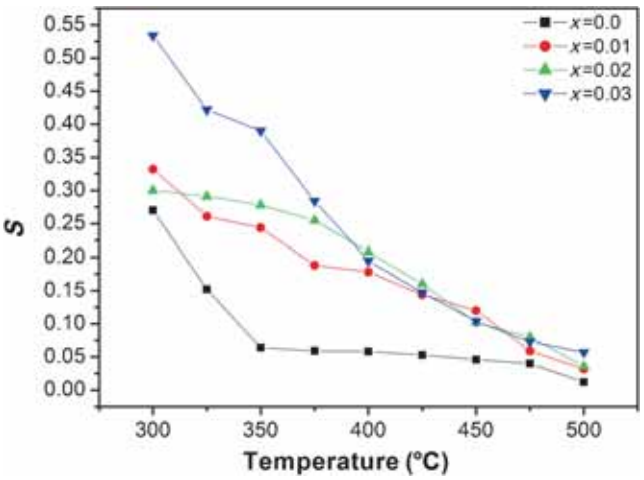

Figure 6. Variation of the frequency exponent s with temperature for $Zn_{1-x}Ca_xO$ nanoceramics.

part shows the peak point at a particular frequency called the resonant frequency. The resonant frequency will increase with increasing measurement temperature due to the control space charge carriers. The frequency-dependent imaginary part shows the relaxation nature. It was also observed that the value of Z'' increases with increase in concentration of Ca.

The frequency-dependent conductivity increases approximately linearly with frequency as $\sigma(\omega) = A\omega^s (0 < s < 1)$ [27] and the values of the frequency exponent (s) were calculated for the investigated nanoceramics of different compositions from the slope of the linear lines of $\ln(\sigma_{a.c.}(\omega))$ *vs.* $\ln(\omega)$. Figure 6 shows the variation of s with the temperature and the dependence of variation of s values on temperature is a strong evidence for thermally activated polarization mechanism [19]. The values of s show a decreasing trend for all the compositions with increase in temperature. Again the values of s are higher in Ca-doped ZnO than pure ZnO. It has been observed that s is related to doping and stoichiometry of nanoceramics. From figure 6, it is noticeable that values of s are less than unity. They are associated with charge carriers or with extrinsic dipoles arising from the presence of defects or impurities [27].

4. Conclusion

This work reports the results of investigation on the structural and electrical properties of $Zn_{1-x}Ca_xO$ nanoceramics prepared by solid-state reaction method using CIS technique. Structural analysis of the synthesized material suggests that they exhibit a single phase with hexagonal wurtzite structure. The results have shown that the material showed temperature-dependent relaxation phenomena. The dielectric constant of pure ZnO is higher than those of doped samples. Again the doped sample shows dielectric loss at lower temperature than that of the pure sample. It was observed from the result of investigation that Ca-doped ZnO nanoceramics are suitable for electronic and electrical applications.

References

[1] Janotti A and Van de Walle C G 2009 *Rep. Prog. Phys.* **72** 126501

[2] Samuel M S, Koshy J, Chandran A and George K C 2011 *Physica B* **406** 3023

[3] Biju V and Khaddar M A 2001 *J. Mater. Sci.* **36** 5779

[4] Singhal S, Kaur J, Namgyal T and Sharma R 2012 *Physics B* **407** 1223

[5] Hamud A S H, Karthikeyan C, Sasikumar S, Kumar V S, Kumareson S and Ravi G 2013 *J. Mater. Chem. B* **1** 5950

[6] Karthikeyan B, Pandiyarajan T and Mangaiyarkarasi K 2011 *Spectrochim. Acta Part A*: *Mol. Biomol. Spectrosc.* **82** 97

[7] Water W and Yang Y S 2006 *Sens. Actuators A* **127** 360

[8] Chakrabati P, Jit S and Pandey A 2009 *International conference on emerging trends in electronic and photonic devices and systems, Macmillan Advanced Research Series,* Banaras Hindu University, Varanasi, India, 22–24 December (India: Macmillan Publishers India Limited)

[9] Barsoukov E and Macdonald J R (eds) 2005 *Impedance spectroscopy*: *theory*, *experiment*, *and applications*, 2nd edn (New York: John Wiley & Sons Inc.)

[10] Barranco A P, Pinar F C, Martinez O P, Guerra D L S and Carmenate G 1999 *J. Eur. Ceram. Soc.* **19** 2677

[11] Muthukumarn S and Gopalkrishan R 2012 *Opt. Mater.* **34** 1946

[12] Ozgur U, Alivov Ya I, Liu C, Teke A, Reshchikov M A, Dogan S, Avrutin V, Cho J S and Morkoc H 2005 *J. Appl. Phys.* **98** 041301

[13] Bai L N, Lian J S, Zheng W T and Jiang Q 2012 *Cent. Eur. J. Phys.* **10** 1144

[14] Li D, Huang J F, Cao L Y, Li J Y, Yang H B O and Yao C Y 2014 *Ceram. Int.* **40** 2647

[15] Kumar S, Kaur P, Chen C L, Thengavel R, Dong C L, Ho Y K, Lee J F, Chan T S, Chen T K, Mok B H, Rao S M and Wu M K 2014 *J. Alloys Compd.* **588** 705

[16] Romeo S L, Jimenez M J Q, Garia M H and Castillo A A 2014 *World J. Condens. Matter Phys.* **4** 27

[17] Linhua X, Xiao S, Zhang C, Zheng G, Su J and Wang Z L 2014 *J. Mater. Chem. Phys.* **148** 720

[18] Ghosh A, Kumari N, Tewari S and Bhattacherjee A 2015 *Mater. Sci. Eng. B* **196** 7

[19] Ansari S A, Nisar A, Fatma B, Khan W, Chaman M, Azam A and Naqvi A H 2012 *Mater. Res. Bull.* **47** 4161

[20] Parashar S K S, Choudhury R N P and Murty B S 2004 *Mater. Sci. Eng. B* **110** 58

[21] Kamba S, Bovtun V, Petzelt J, Rychetsky I, Mizaras R, Banys B A J, Grigas J and Kosec M 2000 *J. Phys. Condens. Matter* **12** 497

[22] Ansari S A, Nisar A, Fatma B, Khan W, Chaman M, Azam A and Naqvi A H 2012 *Mater. Res. Bull.* **47** 4161

[23] Parashar S K S, Choudhary R N P and Murty B S 2005 *Ferroelectrics* **325** 65

[24] Nadeem M, Akhtar M J, Khan A Y, Shaheen R and Haque M N 2002 *Chem. Phys. Lett.* **366** 433

[25] Sahoo P S, Panigrahi A, Patri S K and Choudhary R N P 2010 *Bull. Mater. Sci.* **33** 129

[26] Das P R, Pati B, Sutar B C and Choudhury R N P 2012 *Adv. Mater. Lett.* **3** 8

[27] Bharadwaja S S N, Victor P, Venkateswarulu P and Krupanidhi S B 2002 *Phys. Rev. B* **65** 174106